HHS Public Access

Author manuscript

J Neural Eng. Author manuscript; available in PMC 2016 August 01.

Published in final edited form as:

J Neural Eng. 2015 August ; 12(4): 046022. doi:10.1088/1741-2560/12/4/046022.

Isolating gait-related movement artifacts in electroencephalography during human walking

Julia E. Kline[1,*], **Helen J. Huang**[2], **Kristine L. Snyder**[2], and **Daniel P. Ferris**[1,2]

[1]Department of Biomedical Engineering, University of Michigan, Ann Arbor, MI

[2]School of Kinesiology, University of Michigan, Ann Arbor, MI

Abstract

Objective—High-density electroencephelography (EEG) can provide insight into human brain function during real-world activities with walking. Some recent studies have used EEG to characterize brain activity during walking, but the relative contributions of movement artifact and electrocortical activity have been difficult to quantify. We aimed to characterize movement artifact recorded by EEG electrodes at a range of walking speeds and to test the efficacy of artifact removal methods. We also quantified the similarity between movement artifact recorded by EEG electrodes and a head-mounted accelerometer.

Approach—We used a novel experimental method to isolate and record movement artifact with EEG electrodes during walking. We blocked electrophysiological signals using a nonconductive layer (silicone swim cap) and simulated an electrically conductive scalp on top of the swim cap using a wig coated with conductive gel. We recorded motion artifact EEG data from nine young human subjects walking on a treadmill at speeds from 0.4–1.6 m/s. We then tested artifact removal methods including moving average and wavelet-based techniques.

Main Results—Movement artifact recorded with EEG electrodes varied considerably, across speed, subject, and electrode location. The movement artifact measured with EEG electrodes did not correlate well with head acceleration. All of the tested artifact removal methods attenuated low-frequency noise but did not completely remove movement artifact. The spectral power fluctuations in the movement artifact data resembled data from some previously published studies of EEG during walking.

Significance—Our results suggest that EEG data recorded during walking likely contains substantial movement artifact that: cannot be explained by head accelerations; varies across speed, subject, and channel; and cannot be removed using traditional signal processing methods. Future studies should focus on more sophisticated methods for removing of EEG movement artifact to advance the field.

Keywords

EEG; gait; movement artifact; moving average; wavelets

Correspondence: Julia Kline, Human Neuromechanics Laboratory, 401 Washtenaw Ave, Ann Arbor, MI, 48108, USA, jekline@umich.edu.

1. Introduction

Measuring brain activity during human walking has the potential to advance both basic neuroscience and functional technologies. Imaging the brain during movement can help determine what brain areas are involved in neuromotor control and how they interact during motor activities. Further, real-time information about brain processes during everyday activities as people walk could allow for the design of more broad-ranging brain machine interfaces. In addition, mobile brain imaging devices would provide valuable information about the brain activity patterns of individuals with neural disorders. For these goals to be achieved during locomotion, it is imperative to: 1) be able to identify specific brain sources, which requires good spatial resolution, 2) be able to observe split-second neural changes within a stride, which requires good temporal resolution, and 3) be able to extract strictly neural signals.

Advanced electroencephalography (EEG) technologies allow for novel insight into human brain function during whole-body movements. EEG has inherently good (millisecond) temporal resolution, and inverse source modeling techniques can provide spatial localization in the range of 1 cm (Makeig et al., 1996; Makeig et al., 2004a; Makeig et al., 2004b; Mullen et al., 2011). Functional near-infrared spectroscopy (fNIRS) has been used to study walking previously (Miyai et al., 2001; Suzuki et al., 2004; Harada et al., 2009), but it relies on a hemodynamic response, which has poorer temporal resolution. EEG offers better temporal resolution than fNIRS (Villringer and Chance, 1997; Irani et al., 2007), because EEG measures fast electrical potential changes rather than a slow metabolic signal. Combined with advanced statistical techniques, EEG can have comparable spatial resolution to fNIRS (Makeig et al., 2004a, Makeig et al., 2004b). Our laboratory has recorded electrocortical spectral fluctuations during treadmill walking in healthy, young adults (Gwin et al., 2011; Sipp et al., 2013). Other groups have also proved the feasibility of measuring scalp electrocortical signals during human walking, at speeds ranging from 0.42 m/s to 1.9 m/s, to provide insight into brain function (Gramann et al., 2010; Cheron et al., 2012; Lau et al., 2012; Severens et al., 2012; Wagner et al., 2012; Seeber et al., 2014; Seeber et al., 2015).

EEG recordings are a mixture of electrocortical and other signals, which ideally need to be separated to examine the brain activity. Other signals recorded by EEG systems include muscle and heart activity, eye movement, line noise, electromagnetic fields, and movement artifact (Figure 1(a); Gwin et al., 2010). To identify and remove these additional signals, first and foremost, researchers can use visual inspection of EEG data to reject channels and time periods with large movement artifacts. There are also relatively simple frequency-based methods for removing artifact. Line noise can be separated by identifying and removing power at a frequency of 50 or 60 Hz. Either all power at this frequency can be removed via a notch filter, or only that which is independent of data at other frequencies. If the primary focus of a study is on non-gait related cognitive tasks, a moving average artifact template can be used to reject movement artifacts (Gwin et al., 2010). The drawback of this technique is that it also removes electrical brain activity that is time-locked to the gait cycle. Wavelet-based cleaning methods have been used in previous EEG studies to identify or remove low-frequency spectral fluctuations (Adeli et al., 2003, Daubechies, 1988).

There are additionally more complex, comprehensive mathematical methods for removing artifact from neural data. Blind source separation techniques, such as Independent Component Analysis (ICA) and Canonical Correlation Analysis (CCA) (Sweeney et al., 2013), have been successful at separating eye and muscular artifacts from EEG data (Jung et al., 2000a; Jung et al., 2000b), but they may be less successful with movement artifact due to the lack of independence between different noise signals. Additionally, Artifact Subspace Reconstruction (ASR) (Mullen et al., 2013) has also been used to remove artifacts from EEG recordings. ASR is a more complex, sophisticated method for movement-related artifact removal, but is beyond the scope of this paper. However, it will be included in a future analysis of how ASR and other more sophisticated techniques work in isolation and in combination to remove gait-related artifact.

Another approach to determining how to separate movement artifacts from scalp EEG during human walking is to focus on characterizing the electrical artifacts induced by gait. Castermans and colleagues recently compared spectral fluctuations over the gait cycle in EEG data and accelerometer data. They found common harmonics in the spectra of the EEG and the accelerometer that roughly corresponded to the subjects' fundamental stepping frequency and increased with speed (Castermans et al., 2014). However, because accelerometers and EEG electrodes measure fundamentally different quantities, gait-related movement artifacts may differ between the two. Small movements of electrodes relative to a subject cause the electrodes to register a change in voltage, whereas the accelerometer only measures changes in the head's acceleration relative to the environment. Using EEG electrodes to quantify artifact induced by head movement during locomotion is also problematic because the EEG will contain a mixture of true electrocortical signals and artifact signals, with no clear way to distinguish the relative contributions of the two. If we could explicitly determine the spectral and temporal properties of the movement artifact, it might be possible to remove the artifact while keeping the real electrocortical content that is synchronized to the gait cycle. However, to truly characterize movement artifact in EEG recordings, we must first isolate it.

The purpose of this study was to isolate, record, and characterize movement artifact in EEG during human walking. We used a nonconductive layer, a silicone swim cap, to block all neural, muscular, ocular, and other physiological signals from the EEG electrodes (Figure 1(a)). While the signal we recorded likely contained nonphysiological electrical signals and movement artifact, the nonphysiological electrical signals, such as line noise and electromagnetic field noise, occur in a narrow frequency band and are small in magnitude, respectively, leaving our data dominated by movement artifact. We therefore refer to the data recorded by the EEG electrodes as movement artifact data. We placed a wig coated with conductive gel over the swim cap to simulate an electrically conductive human scalp with hair. Nine healthy subjects walked on a treadmill over a range of speeds, while we recorded movement artifact data, head accelerations, and kinematic data. We hypothesized that EEG electrodes isolated from any electrophysiological signals would show gait-linked spectral fluctuations that varied across speed. We also tested the ability of a few simple cleaning methods to remove this movement artifact. Characterizing and attenuating walking-related movement artifact in EEG electrodes should improve our ability to study brain dynamics during walking.

2. Material and Methods

2.1 Data Collection

Nine healthy young adults (27.0 +/− 4.8; male=4, female=5) with no known musculoskeletal or neurological deficits participated in the study. The University of Michigan Institutional Review Board approved the study protocol, and all subjects gave written informed consent.

We devised a multi-layer approach to isolate and measure movement artifact with EEG electrodes (Figure 1(b); Active II, BioSemi, Amsterdam, The Netherlands). First, we placed a nonconductive layer, a silicone swim cap, over the subject's scalp. The nonconductive layer prevents electrophysiological signals from propagating to the electrodes. To measure voltage differences generated by movement, the recording electrodes needed to be in contact with a conductive medium. To achieve this, we used a wig that was coated with conductive gel to simulate a scalp with hair. This was placed directly over the swim cap. We then placed the EEG cap over the simulated scalp and gelled the electrodes as customary for EEG studies (Gwin et al. 2011). To view whether the silicone swim cap was blocking electrophysiological signals from the EEG electrodes, we asked subjects to blink their eyes and clench their jaw as we visually inspected the channel data. We ensured that no muscle or eye artifact was visible in the EEG traces. To verify that we were measuring movement artifact, we asked subjects to nod their head up-and-down and shake their head from side-to-side, and we also physically shook the wires as we visually inspected the channel data for movement artifacts. Large movement artifacts were visible in the EEG traces during head movement and shaking for all subjects.

We also estimated how well the resistances of our simulated scalp compared with the resistance of a natural human scalp (~0.001–0.1 Mohm for dry skin, Fish and Geddes, 2003). We used a multimeter to measure the resistances between the ground and the electrodes on the simulated scalp (0.9 ± 0.4 Mohm). We also checked that the BioSemi electrode offsets were <20 mV, as recommended by BioSemi's website (www.biosemi.com). The BioSemi system uses active electrodes, which are designed to reduce current flow through the skin-gel-electrode interface and thus reduce extraneous voltages from changes in impedance related to changes in the skin-gel-sensor interface. The measured multimeter resistances of our simulated scalp and the voltage offsets provided by BioSemi suggest that the electrode characteristics were similar for the simulated scalp and actual human scalp.

Subjects walked on a custom force treadmill at a range of speeds (0.4, 0.8, 1.2, 1.6 m/s) as we recorded movement artifact data, lower limb kinematics, and accelerations of the head (Figure 1C). Subjects walked at each speed for 10 minutes, and we randomized the order of the speeds. We also collected 10 minutes of sitting data at the beginning and end of the walking portion of the experiment. We used a ten-camera motion capture system (Vicon Nexus, Oxford, UK) to record kinematic trajectories of calcaneus markers, one on each foot. We recorded ground reaction forces for each lower limb as subjects walked. For the final six of the nine subjects, we used double-sided tape to place an inertial measuring unit (IMU) with a tri-axial accelerometer (The Opal, APDM, Inc., Portland, OR) on the subject's forehead along the midline of the nose and covered the accelerometer with an additional piece of tape (Figure 1C). We placed the accelerometer on the forehead in order to get the

best estimate of the acceleration of the head without interfering with the movement artifact recorded in any of the EEG channels. We recorded 5 minutes of accelerometer data for each speed. The sampling frequencies were 512 Hz, 100 Hz, 1000 Hz, and 128 Hz for the EEG, motion capture, ground reaction force, and accelerometer data, respectively.

2.2 Data Analyses

We compared the time courses of the accelerometer data, ground reaction forces, and movement artifact signal. We first aligned all of the data to a common trigger, a square wave of a constant frequency sent simultaneously to the different recording systems. We smoothed the ground reaction forces using a moving average of a 50-ms time window.

To analyze the data with respect to the gait cycle, we used the calcaneus markers to identify gait events. We applied a 6 Hz low-pass Butterworth filter to smooth the kinematic data. The gait cycle consisted of the following gait events: initial left toe-off (LTO), left heel-strike (LHS), right toe-off (RTO), right heel-strike (RHS), and the subsequent left toe-off. Heel-strikes corresponded to the times of the troughs of the calcaneus marker vertical position and toe-offs corresponded to the times of the peaks of the calcaneus marker velocity in the vertical direction (Kline et al., 2014).

We processed the EEG movement artifact signals offline using customized MATLAB scripts and EEGLAB (Delorme and Makeig, 2004). We performed initial analyses using all of the electrodes, but eventually focused our analyses on 5 electrodes spatially distributed around the head at the front (E12), back (A19), left (G11), right (C18), and top center (A1). These positions are relative to a BioSemi 256 channel headcap (http://www.biosemi.com/headcap.htm). We high-pass filtered the movement artifact signals using a two-way least squares FIR filter with a cutoff frequency of 1 Hz to remove drift. We divided the data into epochs corresponding to gait cycles, time-locked to left toe-off. To be as consistent as possible with previous published studies, we re-referenced the data to the average of all 256 channels (Gwin et al., 2011; Sipp et al., 2013). We rejected epochs that were greater than 3 standard deviations from the means of the gait event times. We then used the remaining epochs as the raw data that we included in further analyses.

We applied three movement artifact cleaning methods (discussed below) to the movement artifact data. For the uncleaned and the three cleaned data sets, we calculated changes in spectral power relative to baseline (event related spectral perturbations: ERSPs) according to Gwin et al. (Gwin et al., 2011). Briefly, this involved computing a spectrogram for each channel and epoch of data. We time-warped the spectrograms so that the gait events occurred at the same relative time within the gait cycle, to account for differences in absolute timing from stride to stride. We averaged the spectrograms for all epochs for the same channel and condition. To visualize power fluctuations about the baseline frequency spectrum, we subtracted the average frequency spectrum for the whole gait cycle from the frequency spectrum at each time point. We then averaged these ERSPs across all subjects (Makeig 1993; Makeig et al., 2004a). We used bootstrapping methods available in EEGLAB (Delorme and Makeig, 2004) to determine regions of significant difference from baseline ($p < 0.05$).

Furthermore, we wanted to quantify how similar the ERSP plots were across subject, speed, and electrode location. An ERSP is a three dimensional matrix of time by frequency by power, with the power values representing a power change from baseline. We used the Matlab 'corr' function to compute a pairwise linear correlation coefficient for the power values for our ERSP comparisons (Tables 1–2). We focused our analyses on channel A1 and 1.2 m/s. Channel A1 in the BioSemi EEG system is comparable to Cz in a traditional 10–20 system, and is closest to the motor cortex, where we would expect there to be significant activity during walking in a true EEG study. Preferred walking speed is consistently found to be 1.2–1.3 m/s, leading us to focus on 1.2 m/s, the closest walking speed to preferred that we collected.

2.2.1 Movement Artifact Cleaning Methods—We applied three potential artifact cleaning methods: 1) moving average, 2) wavelets, and 3) moving average + wavelets. The first artifact cleaning method we used was a moving average, outlined in (Gwin et al., 2010). For the moving average, we specified the number of time-warped strides to average before and after the current stride and the low-pass filter cutoff frequency to apply to the average stride data. We subtracted this low-pass filtered time-warped average stride data from the raw data for the current stride. We used 10 strides and a 10 Hz low-pass filter cutoff, based on (Gwin et al., 2010). We then detrended the data, as the moving average processing sometimes introduced a linear trend into the data. The second artifact cleaning method was wavelets. Using Daubechies 4 wavelets, we removed signal content at frequencies below 8 Hz and applied the wavelets to the whole stride. The third artifact cleaning method combined the moving average and wavelets. We first applied the moving average (10 strides, 10 Hz cutoff) and then the wavelet method (8 Hz over the whole stride). The moving average method occasionally introduced artifacts (<1% of the epochs). We identified epochs with values above a threshold of 100 μV and rejected them from all files to ensure that all artifact cleaning methods analyzed the same strides.

2.2.2 Accelerometer Analyses—We compared the movement artifact signals measured using the EEG system with the head accelerations in all three directions (vertical, mediolateral, and anterior-posterior) measured using an accelerometer placed on the forehead. We used a fast Fourier transform (FFT) to compute the frequency spectra of each measure for the entire length of the data (EEG frequency resolution: 0.0017 Hz, accelerometer frequency resolution: 0.0033 Hz). We downsampled the movement artifact data recorded with the EEG system to 128 Hz, to match the sampling frequency for the accelerometer. Because there is most likely a time lag between the movement artifact signals recorded in the EEG electrodes and the head acceleration, we calculated the cross-correlation between the time series of each head acceleration direction and each electrode channel. We used MATLAB's xcorr function to find the lag that corresponded with the maximum correlation for each combination of head acceleration direction and electrode channel (3 head acceleration directions x 256 EEG channels). Because the maximum correlations mostly occurred between the vertical head acceleration and movement artifact signals, we shifted the time series data by the lag that corresponded to the maximum correlation between the vertical head acceleration direction and each channel. The lag time used to align the movement artifact signal with the head acceleration was specific to each

channel. We then performed a linear regression using the whole time series (~5 minutes) where an individual channel movement artifact signal was the response and all three head acceleration directions were predictors using MATLAB's fitlm function. We repeated this linear regression analysis for each electrode channel to determine how much of the variation in the movement artifact signal recorded by that specific EEG electrode was due to the accelerations. To examine time-frequency characteristics, we also compared ERSPs for the accelerometer data with the ERSPs for the movement artifact data. To allow for fair comparison, we computed ERSPs for the accelerometer data using the same process described above for the movement artifact data.

2.2.3 Mastoid Experiment: Comparison of Data from Simulated Scalp Interface and Human Skin Interface—To verify that the electrode/simulated scalp interface was fundamentally similar to an electrode/human skin interface, we had one of our nine subjects return for an additional experiment (Figure 8(a)). To obtain movement artifact data for the electrode/simulated scalp interface, we set up the experiment as previously described using the silicone swim cap and wig coated with conductive gel. The subject walked on the treadmill for five minutes at 1.2 m/s while we collected movement artifact data on the simulated scalp interface. To obtain movement artifact data for an electrode/human skin interface, we placed one EEG electrode on the subject's left mastoid, a bony prominence known to have minimal electrophysiological signal. The BioSemi system uses two separate electrodes (common mode sense, CMS, electrode; driven right leg, DRL, electrode) to increase the common mode rejection ratio, instead of using a single ground electrode. There was not enough space on the subject's mastoid to place the EEG electrode and the two BioSemi reference electrodes. We therefore placed the BioSemi CMS reference electrode on the left mastoid, next to the EEG electrode we were recording from, and the DRL reference electrode on the right mastoid. The subject again walked for five minutes at 1.2 m/s while movement artifact data were recorded.

To determine if the two interfaces recorded movement artifact of a similar pattern and magnitude, we applied the ERSP analysis described above to both control datasets. For the electrode/simulated scalp data, we computed ERSP plots for the channels closest to the left mastoid, G21 and G22 (http://www.biosemi.com/headcap.htm). For the electrode/human skin data, we computed an ERSP plot for the electrode placed on the subject's mastoid. We used the correlation method described above to compute a measure of similarity between the simulated scalp and mastoid ERSPs.

3. Results

The EEG electrodes measured movement artifact waveforms that varied across speed and electrode location. Waveforms increased in amplitude as walking speed increased (Figure 2). At the slowest speed, little movement artifact was detected. At the fastest speed, the movement artifact waveforms were more evident. The movement artifact also varied between electrode locations (Figure 2).

The time course waveforms of the head acceleration and movement artifact signals were different (Figure 2). During single support (when only one leg is in contact with the ground),

there was typically a single peak in the accelerometer time series but multiple peaks and valleys in some of the electrode time series. The vertical accelerations of the head did not correlate well with the movement artifact signals measured by the electrodes (Figure 3). A phase space plot of the E12 electrode voltage versus the vertical head acceleration appeared to have no clear relationship across speeds (Figure 3(a)). The correlation coefficients were greatest for the vertical head acceleration and the movement artifact signals recorded in the EEG electrodes compared to the mediolateral and anterior-posterior accelerations (Figure 3(b)). At the normal walking speed (1.2 m/s), the average correlation coefficient was 0.35 ± 0.07 for the vertical, 0.14 ± 0.03 for the mediolateral, and 0.17 ± 0.04 for the anterior-posterior head accelerations. Additionally, the group average correlation coefficients increased with walking speed (Figure 3(b)). For the vertical direction, the average correlation coefficient was 0.18 ± 0.06, 0.37 ± 0.09, 0.35 ± 0.07, and 0.31 ± 0.08, from the slowest (0.4 m/s) to fastest (1.6 m/s) walking speed respectively. The linear regressions using the head accelerations in all three directions had an overall average R-squared of 14.3 ± 0.05, for the 5 primary channels we focused on, and across all speeds (Table 3). This indicates that the head accelerations only account for ~14% of the variance of the movement artifact signal recorded by the EEG electrodes.

Although there was some overlap, particularly for the lower frequencies, the frequency spectra for the accelerometer and the movement artifact data revealed spectral power harmonics at different frequencies and over different frequency ranges. (Figure 4). The accelerometer frequency spectra in the vertical direction had large peak amplitudes up to 20 Hz at the fastest walking speed. The movement artifact frequency spectra and accelerometer frequency spectra in the mediolateral and anterior-posterior directions had large peak amplitudes up to 10 Hz at the fastest walking speed. Movement artifact signal spectra amplitudes increased with faster walking speeds for the head accelerations in all three directions and all the electrodes.

There were different distinctive patterns of movement artifact in the individual subject ERSPs that varied across walking speeds (Figure 5, Table 1). The individual subject ERSPs highlighted that the movement artifact varied from subject to subject. As an example, we quantified the ERSP correlation coefficients across subjects for channel A1 at 1.2 m/s. Average correlation values were low (mean 0.09) and had a high standard deviation (0.11). These values indicated a high inter-subject variability. (For the raw data values, see Table 1 in the supplement). For many of the subjects, the pattern of spectral power change was variable across speeds. We quantified this variability by calculating correlation coefficients (Table 1), which revealed low correlation values when averaged across subjects. Individual subject ERSPs consistently indicated that the magnitude of the movement artifact and the maximum frequency at which it occurred increased with increasing walking speed. The individual subject ERSPs for the vertical head acceleration showed broadband spectral fluctuations, which were not consistently observed in the movement artifact ERSPs for all subjects and speeds (Figure 5).

Additionally, the ERSPs for the different electrode locations showed different patterns of movement artifact, which also varied across walking speed (Figure 6, Tables 1 and 2). Depending on the electrode location, the movement artifact differed, particularly with

respect to the magnitude. The midline electrodes (A1, A19, & E12) generally recorded larger movement artifacts than the lateral electrodes (C18 & G11) (Figure 6). Based on the magnitude of the fluctuations in the ERSPs, the electrode on the front of the head (E12) was the most susceptible to movement artifacts compared with the other electrodes.

There were some consistent patterns across speeds in the ERSPs for individual subjects (Figure 5) and for different electrodes (Figure 6). During the double support period (when both legs are in contact with the ground), there tended to be synchronization in the 8–30 Hz range at the fastest speed (1.6 m/s). At the slowest speed (0.4 m/s), double support tended to show a desynchronization in the 4–7 Hz range. In contrast, during the single support period, there was typically a strong desynchronization at the fastest speeds and a slight desynchronization at the slower speeds. However, correlation coefficient values reveal that these patterns are not completely consistent across all subjects and electrode locations (Tables 1 and 2). The mean ERSP were most highly correlated for the two lowest speeds, 0.4 and 0.8 m/s. However, significant changes in pattern occurred from the slowest to the fastest speed, as evidenced by both the ERSPs and correlation values. Additionally, ERSPs for the accelerometer data in all three directions showed broadband synchronization and desynchronization, in contrast to the ERSPs for the movement artifact (Figure 6).

The moving average, wavelet, and moving average + wavelet cleaning methods attenuated but did not remove all movement artifacts (Figure 7). We found that the cleaning methods had some success attenuating low-frequency, gait-related movement artifact at the slowest speed. Though the moving average and wavelet methods seemed to perform similarly, the combination of both seemingly had modest improvements over either method alone at these slower speeds. However, there was little quantitative difference between the two methods. At the fastest speeds, none of the cleaning methods we examined had much success attenuating the stride-locked movement artifact.

3.1 Mastoid data comparison

The ERSPs from the mastoid experiment indicated that EEG electrodes placed on the simulated scalp interface recorded movement artifact of a similar pattern and magnitude as EEG electrodes placed on human skin (Figure 8B). The mastoid ERSP and the ERSPs for channels G21 and G22 on the simulated scalp showed similar movement artifact magnitude and timing in all but the highest frequencies. The correlation coefficients for the mastoid ERSP and the ERSPs for channels G21 and G22 were 0.54 and 0.57, respectively.

4. Discussion

The main finding of the study was that movement artifact patterns recorded in EEG electrodes during walking had large spectral fluctuations over the gait cycle that increased in amplitude as walking speed increased. As speed increased, not only did the amplitude of the spectral fluctuations increase, but the spectral fluctuations appeared in higher frequency bands. Another important finding was that the movement artifact patterns recorded by the EEG electrodes varied substantially across subjects and among electrodes located at different areas of the head. We applied some simple cleaning methods, moving average and wavelets, to the artifact data, but these cleaning methods were insufficient to remove all

movement artifact. A third key finding of the study was that data from an accelerometer placed on the forehead had poor correlation with the movement artifact recorded by the EEG electrodes. There were substantially different spectral fluctuations between the EEG electrode data and the accelerometer data, however there were some similarities. Above 0.4 m/s the artifact spectral fluctuations were similar to the accelerometer spectral changes at 8–30 Hz for some subjects, but the timing was slightly shifted. Altogether, our findings highlight and quantify limitations in current EEG techniques and data cleaning methods. New approaches need to be developed to account for movement artifact patterns, especially at faster walking speeds, that affect EEG electrode data in order to improve interpretation of electrocortical activity during human locomotion.

Several past studies have found spectral power increases during double support and spectral power decreases during single support at alpha and beta frequencies of scalp EEG at normal walking speeds, 0.78–1.25 m/s (Gwin et al., 2011, Cheron et al., 2012, Severens et al., 2012). These fluctuations have been reported to be caused by neural activity. Our pure movement artifact data, which contains no neural activity, also found that some subjects showed increased spectral power during double support and decreased spectral power during single support at faster walking speeds. This suggests that the spectral fluctuations reported in the previous studies reflect a combination of neural activity and movement artifact. Some studies conducted at faster walking speeds may have reported relatively little neural activity compared to artifact. Other studies at slower walking speeds, 0.22–0.60 m/s, have shown some increases in spectral power during double support in alpha and beta frequencies as well (Sipp et al. 2013; Wagner et al., 2012). However, the magnitude and duration of the increased spectral power at double support in our artifact data appears to be reduced substantially for the slower walking speeds. EEG data recorded at slower speeds are less likely to be contaminated with movement artifacts, especially in the higher frequency bands. Though using slower walking speeds may minimize movement artifact, it may also fundamentally change the motor task from rhythmic walking to a discrete stepping task, and so may limit the conclusions that may be drawn from such a study. Future studies may have to balance minimizing movement artifact with using speeds that are fast enough to be representative of typical human walking.

Simple cleaning methods do not appear to sufficiently attenuate movement artifacts in EEG collected at fast walking speeds. We tested a moving average artifact template that had successfully reduced EEG movement artifact in a study of non-gait related cognitive events during walking and running (Gwin et al. 2010). We also tested Daubechies wavelets as a means to identify and remove low frequency artifact. We chose Daubechies wavelets based on their previous usage in EEG studies to identify low frequency spectral fluctuations (Adeli et al., 2003 Daubechies, 1988). Both the moving average and wavelet artifact cleaning methods performed similarly in our study, but substantial movement artifacts remained at faster speeds (Figure 7). Consistent with previous results, the moving average worked well for removing artifacts that had a consistent pattern across occurrences (Chowdhury et al., 2014). Because stride to stride changes in movement patterns lead to differences in movement artifact, this cleaning method could only remove the noise that was consistent from stride to stride. In addition to the results presented, we also tested other values of stride numbers (±3 strides) and filter cutoff frequencies (30 Hz) for the moving average template.

There were no noticeable differences between the other values tested and the ones used for the current figures. The moving average template did tend to exacerbate electrical line noise (60 Hz) (Figure 7). The wavelet filter was less computationally expensive but eliminated almost all information below a given frequency (Figure 7). As a result, wavelets are not useful for targeting gait-related movement artifact and retaining low frequency electrocortical activity.

EEG studies that use cognitive tasks that are not synchronized to the gait cycle are much less likely to have data interpretation affected by movement artifacts. For example, using a visual oddball task or another cognitive task that is not synchronized to the gait cycle allows for any movement related artifacts (and true electrocortical activity synchronized to the gait cycle) to wash out over a large number of cognitive events (Gwin et al., 2010; Gramann et al., 2010; Kline et al., 2014). For future research examining electrocortical activity during human locomotion, it would be beneficial to include a repetitive cognitive event non-synchronized to the gait cycle for analysis of EEG data.

Our results indicate that an accelerometer does not record the same movement artifact signal that EEG electrodes record. Past studies have used accelerometers to measure movement artifacts in non-ambulatory tasks such as nodding and shaking of the head (O'Regan et al., 2013; O'Regan and Marnane, 2013; Sweeney et al., 2010). More recently, Castermans et al. used head-mounted accelerometers during walking and found patterns of synchronization and desynchronization in the data, especially at faster walking speeds (Castermans et al., 2014). Our results showed that movement patterns varied substantially across speed, subject, and electrode placement. There was greater complexity and variation than could be described by the simple patterns of desynchronization and synchronization found in accelerometer data. We also found that the accelerometer data did not correlate well with the movement artifact data recorded by our simulated scalp electrodes. Small movement differences between the accelerometer, the electrodes, and their respective wires may contribute to the differences between the movement artifact in the accelerometer data and electrode data. Even with a wireless EEG system, it is possible that the relative motion of the electrodes to the scalp could still generate movement artifacts. The electrodes likely move side-to-side and up-and-down relative to the scalp or simulated scalp, which may lead to voltage drops. Passive electrodes are more susceptible to sudden changes in impedance and capacitance that can lead to sudden changes in voltage. Active electrodes like the ones used in this study may be less susceptible to sudden changes in voltage because active electrodes likely have more stable impedances, which can be observed in real-time in the Biosemi software program as stable voltage offset values.

Although our simulated scalp does not have exactly the same mechanical properties of real human scalp, the comparison of mastoid data and simulated scalp data suggests that it is close enough to capture similar movement artifact waveforms (Figure 8). The two sets of ERSPs are strongly correlated. However, there are substantive differences between the mastoid ERSPs and simulated scalp ERSPs at higher frequencies. The hair fibers of the wig likely provided some damping effect on the movement of the electrode. This could have attenuated the movement artifact recorded by the simulated scalp electrodes at the highest frequencies.

The most accurate approach for recording movement artifact signals in EEG may be to block the electrophysiological signals in some electrodes during data collection so that those electrodes record only the movement artifact. An EEG system that simultaneously measured movement artifact and movement artifact plus neural signal would allow for an interpolative subtraction process that could remove the movement artifact in real-time. This method would not need to rely on data averaged over time and might even be able to be employed in an ongoing basis during data collection. Movement artifact subtraction performed in real-time would advance mobile brain imaging and brain-computer interfaces substantially compared to the current status quo. An interpolative subtraction process would be useful when recording EEG during any full body movement where substantial artifacts occur, including with patient populations with spasticity or other movement disorders.

Chowdury et al. recently explored the possibility of using an interpolative subtraction process to attenuate magnetic resonance imaging (MRI) noise from EEG recordings. They used a reference layer with similar conductivity to the human head to allow subtraction of movement-related and MRI-related artifacts during simultaneous EEG-fMRI recordings (Chowdury et al., 2014). They explored only small (≤7 mm) head movements rather than larger head movements that are more characteristic of human gait. Their reference layer consisted of an agar, water, and sodium mixture that was not very durable. This idea has potential for separating movement artifact from EEG signals in walking, but further work needs to be done to modify the approach for walking applications.

Our study had a few limitations that prevent us from drawing broader conclusions about the relationship between movement artifact and EEG data recordings. First, there was substantial inter-subject variability in the movement artifact signal. This inter-subject variability may have been due to individual gait patterns, electrode cap fit, and/or differences in the preparation of the wig set up for each subject. There was also variability across subjects in head shape, head size, and hair characteristics. All of these head and hair properties could have led to differences in pressure between the electrodes and the scalp. In our preparation, the swim cap did not lay perfectly smooth over the subject’s head. This swim cap effect may also have contributed to the variability we observed across subjects and electrodes. Additionally, our conductive wig preparation had resistances greater than the resistances reported for dry skin. Designing a conductive scalp with resistive properties that more closely match actual scalp may improve the quality of the isolated movement artifact recorded in the EEG electrodes. Despite these limitations, this simple method for isolating and measuring the movement artifact recorded in the EEG electrodes seems to be promising for capturing gait-induced movement artifacts in EEG.

5. Conclusion

The relative amounts of true electrocortical signal and movement artifact in scalp EEG collected during human locomotion is difficult to determine. We created a novel approach for isolating pure movement artifact with EEG electrodes. The results from our simulated scalp protocol indicate that gait-related movement artifact can have varying magnitudes and patterns across subjects, conditions, electrodes, and strides. These differences are more complex than can be captured merely by accelerometry or eliminated by simple artifact

cleaning techniques. The similar patterns of spectral fluctuation in our purely artifactual data and in previous studies of neural activity during walking suggest that the results of those studies need to be interpreted with caution. One possibility for future studies is to simultaneously measure movement artifact so that it can be characterized and removed from the neural data recorded by EEG. Ultimately, designing more sophisticated techniques that target gait-related artifact for individual strides would allow for more complete gait-related movement artifact attenuation in EEG recordings during walking, which could greatly improve brain-machine interfaces and neurorehabilitation technologies.

Supplementary Material

Refer to Web version on PubMed Central for supplementary material.

Acknowledgments

This work was supported in part by Army Research Laboratory (ARL; W911NF-10-2-0022), the National Institutes of Health (NIH; R01 NS-073649), and the National Science Foundation through a Graduate Research Fellowship to Julia Kline and a Postdoctoral Fellowship in Biology to Kristine Snyder (NSF; dBI-1202720) We would like to thank Bryan Schlink and Maggie Smith for help with data collection. We would also like to thank Dr. Cindy Chestek for inspiring the novel collection method.

References

Adeli H, Zhou Z, Dadmehr N. Analysis of EEG records in an epileptic patient using wavelet transform. J Neurosci Methods. 2003; 123:69–87. [PubMed: 12581851]

Browning RC, Baker EA, Herron JA, Kram R. Effects of obesity and sex on the energetic cost and preferred speed of walking. J Appl Physiol. 2006; 100:2, 390–398. DOI: 10.1152/japplphysiol.00767.2005

Castermans T, Duvinage M, Cheron G, Dutoit T. About the cortical origin of the low-delta and high-gamma rhythms observed in EEG signals during treadmill walking. Neurosci Lett. 2014; 561:166–170. DOI: 10.1016/j.neulet.2013.12.059 [PubMed: 24412128]

Cheron G, Duvinage M, De Saedeleer C, Castermans T, Bengoetxea A, Petieau M, Seetharaman K, Hoellinger T, Dan B, Dutoit T, Sylos Labini F, Lacquaniti F, Ivanenko Y. From spinal central pattern generators to cortical network: integrated BCI for walking rehabilitation. Neural Plast. 2012; : 375148.doi: 10.1155/2012/375148 [PubMed: 22272380]

Chowdhury ME, Mullinger KJ, Glover P, Bowtell R. Reference layer artefact subtraction (RLAS): a novel method of minimizing EEG artefacts during simultaneous fMRI. Neuroimage. 2014; 84:307–319. DOI: 10.1016/j.neuroimage.2013.08.039 [PubMed: 23994127]

Daubechies I. Orthonormal bases of compactly supported wavelets. Communications on pure and applied mathematics. 1988; 41:909–996.

Delorme A, Makeig S. EEGLAB: an open source toolbox for analysis of single-trial EEG dynamics including independent component analysis. J Neurosci Methods. 2004; 134:9–21. DOI: 10.1016/j.jneumeth.2003.10.009 [PubMed: 15102499]

Fish, RM.; Geddes, LA. Medical and Bioengineering Aspects of Electrical Injuries. Tucson: Lawyers & Judges Publishing Company, Inc; 2003.

Gramann K, Gwin JT, Bigdely-Shamlo N, Ferris DP, Makeig S. Visual evoked responses during standing and walking. Front Hum Neurosci. 2010; 4:202.doi: 10.3389/fnhum.2010.00202 [PubMed: 21267424]

Gwin JT, Gramann K, Makeig S, Ferris DP. Removal of movement artifact from high-density EEG recorded during walking and running. J Neurophysiol. 2010; 103:3526–3534. DOI: 10.1152/jn.00105.2010 [PubMed: 20410364]

Gwin JT, Gramann K, Makeig S, Ferris DP. Electrocortical activity is coupled to gait cycle phase during treadmill walking. Neuroimage. 2011; 54:1289–1296. DOI: 10.1016/j.neuroimage.2010.08.066 [PubMed: 20832484]

Harada T, Miyai I, Suzuki M, Kubota K. Gait capacity affects cortical activation patterns related to speed control in the elderly. Exp Brain Res. 2009; 193:445–454. DOI: 10.1007/s00221-008-1643-y [PubMed: 19030850]

Irani F, Platek SM, Bunce S, Ruocco AC, Chute D. Functional near infrared spectroscopy (fNIRS): an emerging neuroimaging technology with important applications for the study of brain disorders. Clin Neuropsychol. 2007; 21:9–37. DOI: 10.1080/13854040600910018 [PubMed: 17366276]

Jung TP, Makeig S, Humphries C, Lee TW, Mckeown MJ, Iragui V, Sejnowski TJ. Removing electroencephalographic artifacts by blind source separation. Psychophysiology. 2000a; 37:163–178. [PubMed: 10731767]

Jung TP, Makeig S, Westerfield M, Townsend J, Courchesne E, Sejnowski TJ. Removal of eye activity artifacts from visual event-related potentials in normal and clinical subjects. Clin Neurophysiol. 2000b; 111:1745–1758. [PubMed: 11018488]

Komaromy AM, Brooks DE, Dawson WW, Kallberg ME, Ollivier FJ, Ofri R. Technical issues in electrodiagnostic recording. Vet Ophthalmol. 2002; 5:85–91. [PubMed: 12071864]

Kline JE, Poggensee K, Ferris DP. Your brain on speed: cognitive performance of a spatial working memory task is not affected by walking speed. Front Hum Neurosci. 2014; 8:288.doi: 10.3389/fnhum.2014.00288 [PubMed: 24847239]

Lau TM, Gwin JT, Mcdowell KG, Ferris DP. Weighted phase lag index stability as an artifact resistant measure to detect cognitive EEG activity during locomotion. J Neuroeng Rehabil. 2012; 9:47.doi: 10.1186/1743-0003-9-47 [PubMed: 22828128]

Makeig S, Debener S, Onton J, Delorme A. Mining event-related brain dynamics. Trends Cogn Sci. 2004a; 8:204–210. DOI: 10.1016/j.tics.2004.03.008 [PubMed: 15120678]

Makeig S, Delorme A, Westerfield M, Jung TP, Townsend J, Courchesne E, Sejnowski TJ. Electroencephalographic brain dynamics following manually responded visual targets. PLoS Biol. 2004b; 2:e176.doi: 10.1371/journal.pbio.0020176 [PubMed: 15208723]

Makeig S, Bell AJ, Jung TP, Sejnowski TJ. Independent component analysis of electroencephalographic data. Adv Neural Inf Process Syst. 1996; 8:145–151.

Makeig S. Auditory event-related dynamics of the EEG spectrum and effects of exposure to tones. Electroencephalogr Clin Neurophysiol. 1993; 86:283–293. [PubMed: 7682932]

Miyai I, Tanabe HC, Sase I, Eda H, Oda I, Konishi I, Tsunazawa Y, Suzuki T, Yanagida T, Kubota K. Cortical mapping of gait in humans: a near-infrared spectroscopic topography study. Neuroimage. 2001; 14:1186–1192. DOI: 10.1006/nimg.2001.0905 [PubMed: 11697950]

Mullen, T.; Kothe, K.; Chi, YM.; Ojeda, A.; Kerth, T.; Makeig, S.; Jung, TP. Real-time estimation and 3D visualization of source dynamics and connectivity using wearable EEG. Proceedings of the 35th Annual International Conference of the IEEE Engineering in Biology & Medicine Society; Osaka, Japan. 2013.

Mullen T, Acar ZA, Worrell G, Makeig S. Modeling cortical source dynamics and interactions during seizure. Conf Proc IEEE Eng Med Biol Soc. 2011; :1411–1414. DOI: 10.1109/IEMBS.2011.6090332 [PubMed: 22254582]

O'Regan S, Faul S, Marnane W. Automatic detection of EEG artefacts arising from head movements using EEG and gyroscope signals. Med Eng Phys. 2013; 35:867–874. DOI: 10.1016/j.medengphy.2012.08.017 [PubMed: 23018030]

O'Regan S, Marnane W. Multimodal detection of head-movement artefacts in EEG. J Neurosci Methods. 2013; 218:110–120. DOI: 10.1016/j.jneumeth.2013.04.017 [PubMed: 23685269]

Seeber M, Scherer R, Wagner J, Solis-Escalante T, Müller-Putz GR. EEG beta suppression and low gamma modulation are different elements of human upright walking. Front Hum Neurosci. 2014; 8:485.doi: 10.3389/fnhum.2014.00485 [PubMed: 25071515]

Seeber M, Scherer R, Wagner J, Solis-Escalante T, Müller-Putz GR. High and low gamma EEG oscillations in central sensorimotor areas are conversely modulated during the human gait cycle. Neuroimage. 2015; 112:318–26. DOI: 10.1016/j.neuroimage.2015.03.045 [PubMed: 25818687]

Severens M, Nienhuis B, Desain P, Duysens J. Feasibility of measuring event related desynchronization with electroencephalography during walking. Conf Proc IEEE Eng Med Biol Soc. 2012; :2764–2767. DOI: 10.1109/EMBC.2012.6346537 [PubMed: 23366498]

Sipp AR, Gwin JT, Makeig S, Ferris DP. Loss of balance during balance beam walking elicits a multifocal theta band electrocortical response. J Neurophysiol. 2013; 110:2050–2060. DOI: 10.1152/jn.00744.2012 [PubMed: 23926037]

Sweeney KT, McLoone SF, Ward TE. The use of ensemble empirical mode decomposition with canonical correlation analysis as a novel artifact removal technique. IEEE Trans Biomed Eng. 2013; 60(1):97–105. DOI: 10.1109/TBME.2012.2225427 [PubMed: 23086501]

Sweeney KT, Leamy DJ, Ward TE, Mcloone S. Intelligent artifact classification for ambulatory physiological signals. Conf Proc IEEE Eng Med Biol Soc. 2010; :6349–6352. DOI: 10.1109/IEMBS.2010.5627285 [PubMed: 21096690]

Suzuki M, Miyai I, Ono T, Oda I, Konishi I, Kochiyama T, Kubota K. Prefrontal and premotor cortices are involved in adapting walking and running speed on the treadmill: an optical imaging study. Neuroimage. 2004; 23:1020–1026. DOI: 10.1016/j.neuroimage.2004.07.002 [PubMed: 15528102]

Villringer A, Chance B. Non-invasive optical spectroscopy and imaging of human brain function. Trends Neurosci. 1997; 20:435–442. [PubMed: 9347608]

Wagner J, Solis-Escalante T, Grieshofer P, Neuper C, Muller-Putz G, Scherer R. Level of participation in robotic-assisted treadmill walking modulates midline sensorimotor EEG rhythms in able-bodied subjects. Neuroimage. 2012; 63:1203–1211. DOI: 10.1016/j.neuroimage.2012.08.019 [PubMed: 22906791]

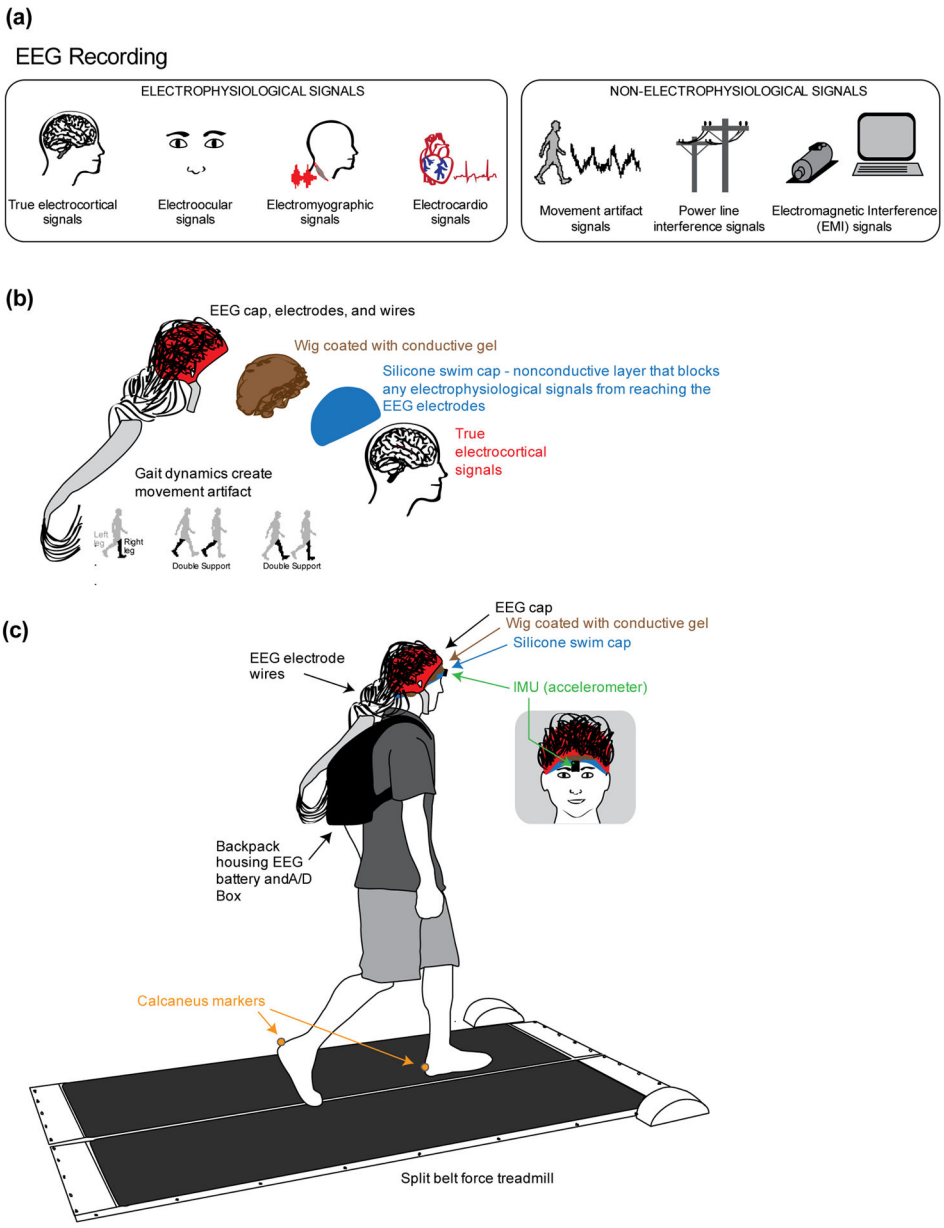

Figure 1.

Conceptual schematic and experimental set up. a) All of the signals that contribute to scalp EEG recordings, categorized as electrophysiological or non-electrophysiological. b) Schematic of the methodological concept for isolating and measuring gait-induced movement artifact in EEG recordings. A silicone swim cap blocks true electrocortical signals while a simulated conductive scalp and a conductive wig allows the electrodes to measure voltage differences resulting from gait dynamics. c) Schematic of the experimental setup. Subjects walked at 4 speeds (0.4, 0.8, 1.2, and 1.6 m/s) on a custom split-belt force measuring treadmill. Trajectories of the calcaneus markers were recorded. An inertial measuring unit (IMU) with a tri-axial accelerometer placed on the forehead above the nose measured accelerations of the head during walking.

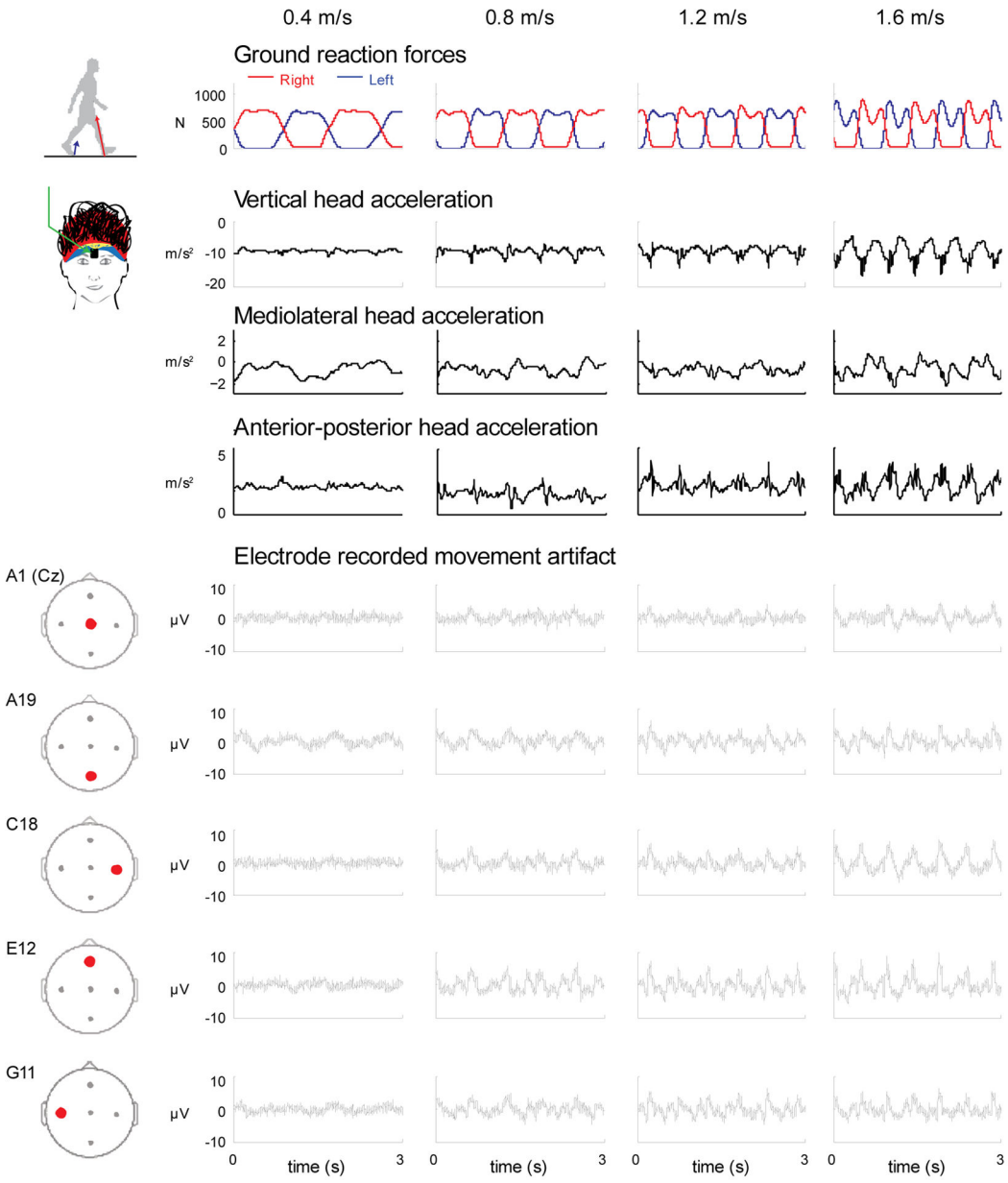

Figure 2.

Time courses of movement artifact and accelerometer data. Time courses of the ground reaction forces for the right and left legs, head accelerations (vertical, mediolateral, and anterior-posterior), and movement artifacts recorded in 5 electrodes (A1, A19, C18, E12, and G11) for the 4 walking speeds (0.4, 0.8, 1.2, and 1.6 m/s) for a single subject.

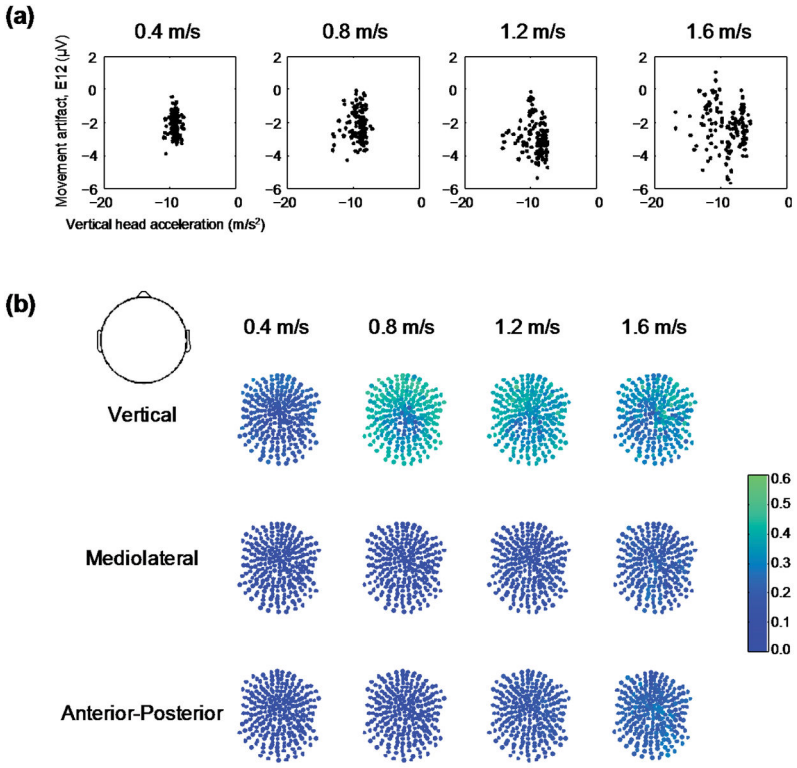

Figure 3.

Correlations between accelerometer and the frontal electrode movement artifact. a) Vertical head acceleration was plotted against movement artifact recorded in the frontal electrode (E12) for a stride of data for a single subject (same data as in Figure 2). b) Correlation coefficients between all three head accelerations and each electrode recorded movement artifact signals were generally < 0.4. Dark blue represents uncorrelated signals, correlation coefficient = 0.0 and green equals a correlation coefficient of 0.6.

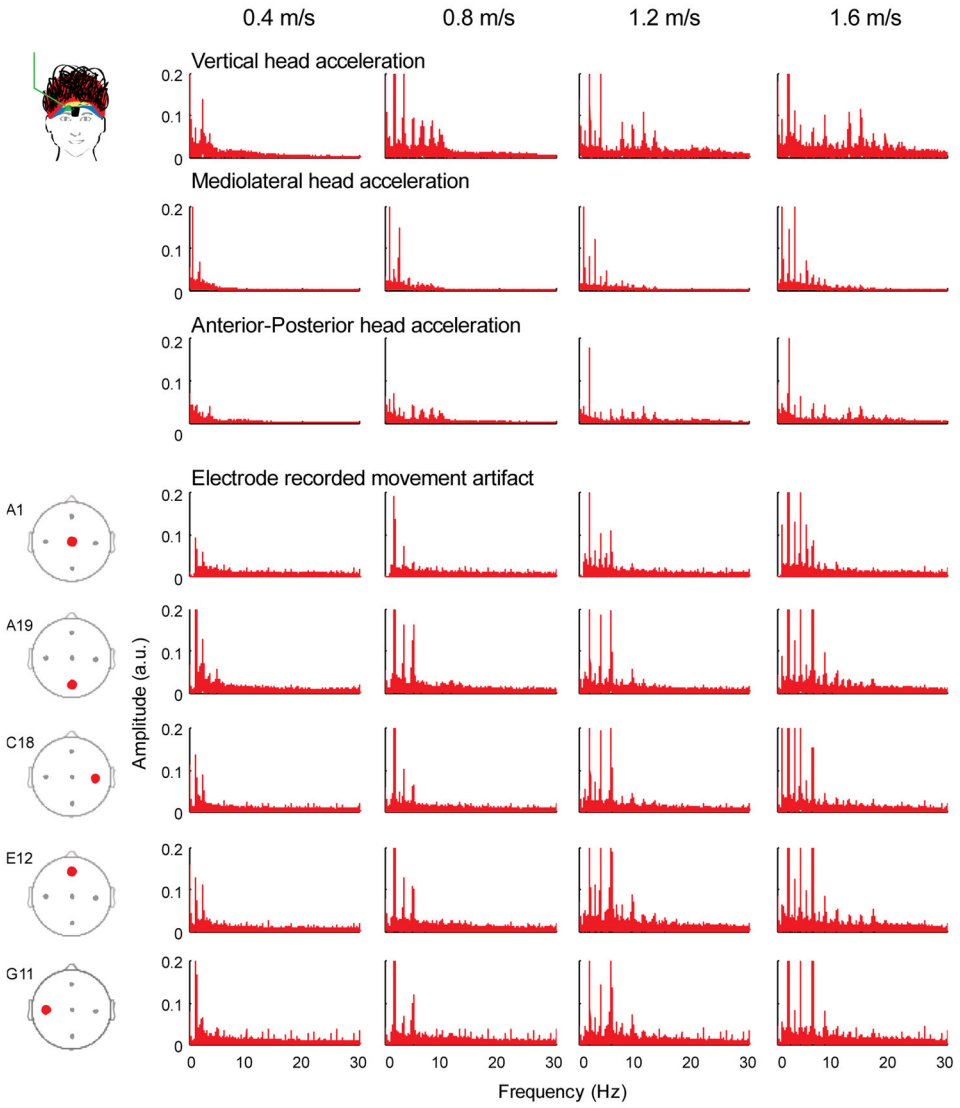

Figure 4.

Frequency spectra for the accelerometer and electrode movement artifacts. Frequency spectra of the head accelerations (vertical, mediolateral, and anterior-posterior) differed from the spectra of the electrode recorded movement artifacts (A1, A19, C18, E12, & G11). Each column is a walking speed, increasing from left to right.

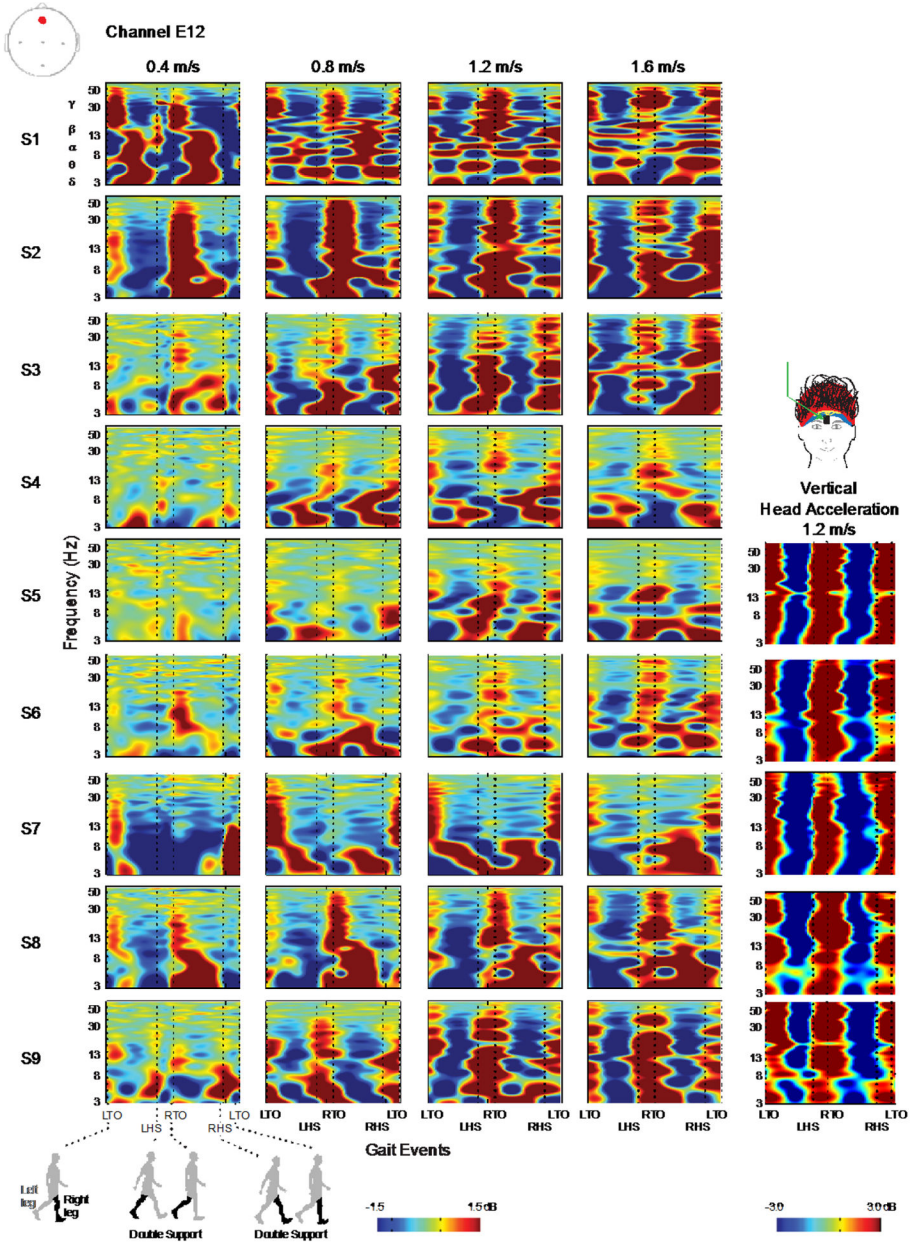

Figure 5.

ERSP plots for individual subjects for both the head mounted accelerometer and channel A1. ERSP plots for individual subjects at channel A1 reveal inter-subject variability in the movement artifact data. ERSP plots of individual subject accelerometer data show that an accelerometer captures less inter-subject variation. Each row is a subject and each column is a walking speed, increasing from left to right. Red represents a power increase from baseline, and blue represents a power decrease from baseline. The x-axis is one gait cycle: left toe-off (LTO), left heel-strike (LHS), right toe-off (RTO), right heel-strike (RHS), and left toe-off again. Double support occurs between the dotted lines of LHS and RTO and between RHS and LTO. Note the different y axes and color bar power scales.

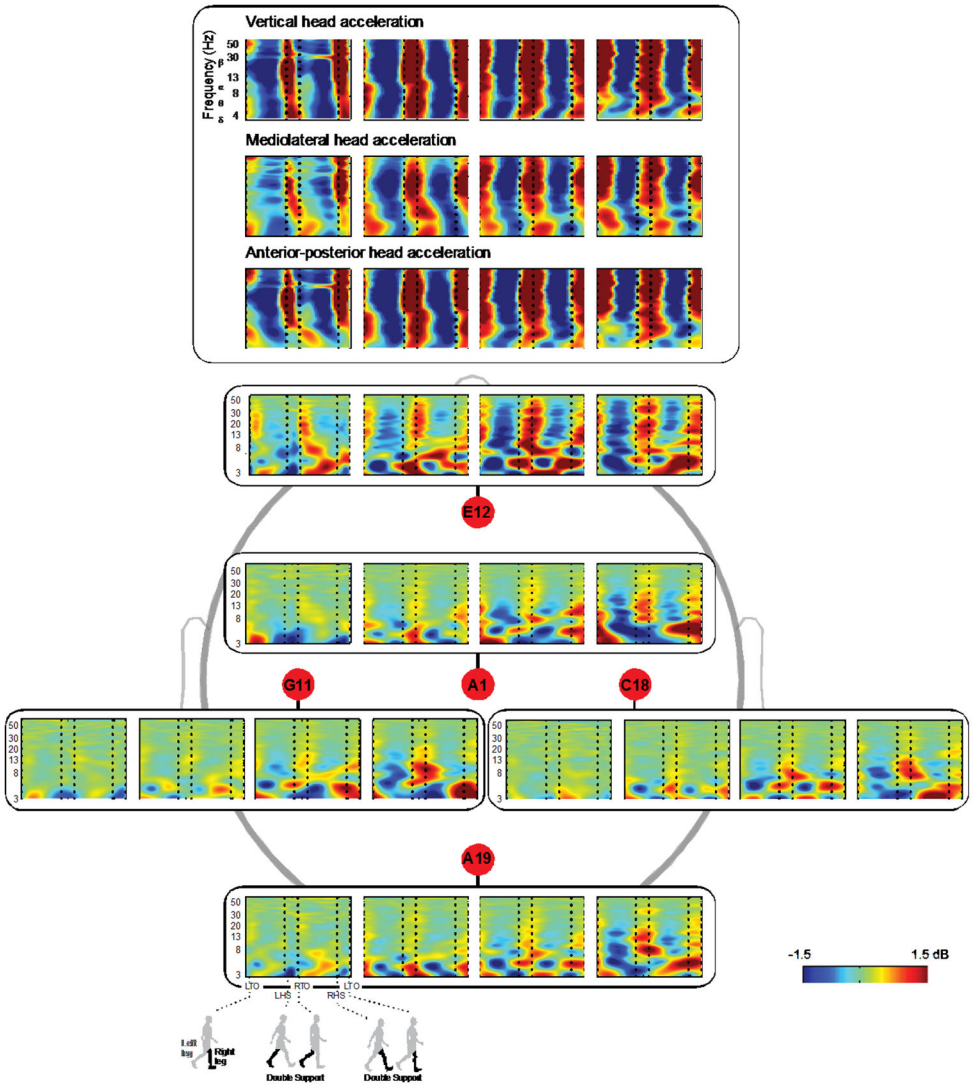

Figure 6.

Group averaged ERSP plots oriented with respect to the head. ERSPs for the head accelerations in all three directions (vertical, mediolateral, and anterior-posterior) showed similar broadband synchronization and desynchronization patterns. ERSPs of the electrode-recorded movement artifact plotted spatially illustrate that midline electrodes (A1, A19, & E12), particularly in the front of the head (E12), were more susceptible to movement artifacts than lateral electrodes (C18 & G11). Red represents a power increase from baseline, and blue represents a power decrease from baseline. Each plot for each electrode is a walking speed, increasing from left to right. The x-axis is one gait cycle: left toe-off (LTO), left heel-strike (LHS), right toe-off (RTO), right heel-strike (RHS), and left toe-off again. Double support occurs between the dotted lines of LHS and RTO and between RHS and LTO.

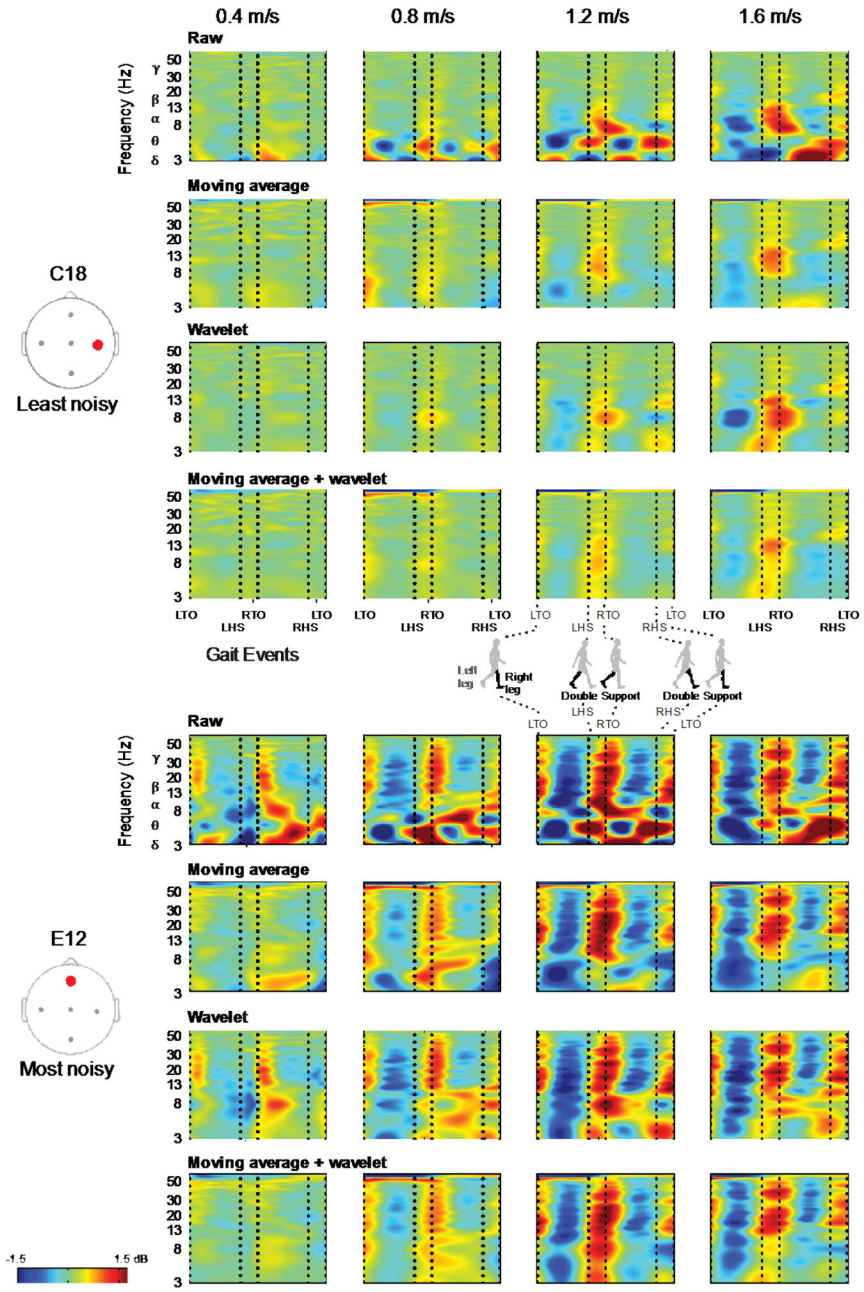

Figure 7.

Group averaged cleaned ERSP plots. Group averaged ERSP plots of the moving average, wavelet, and moving average + wavelet cleaning methods reveal that movement artifact remained despite cleaning. The cleaning results for the least noisy (C18) and most noisy (E12) channels are shown. Each row is a cleaning method and each column is a walking speed, increasing from left to right. Red represents a power increase from baseline, and blue represents a power decrease from baseline. The x-axis is one gait cycle: left toe-off (LTO), left heel-strike (LHS), right toe-off (RTO), right heel-strike (RHS), and left toe-off again.

Double support occurs between the dotted lines of LHS and RTO and between RHS and LTO.

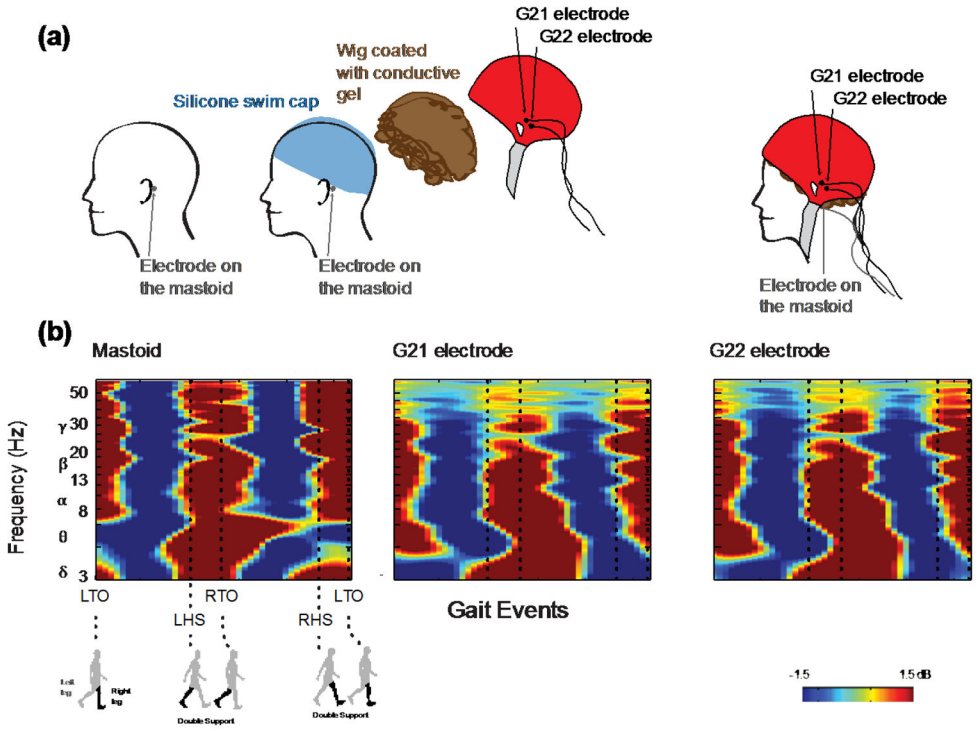

Figure 8.

Schematic of the setup and ERSP plots for the mastoid experiment. **a)** To examine the electrode/human skin interface, an electrode was placed on the left mastoid underneath the swim cap. To examine the electrode/simulated scalp interface, the two electrodes closest to the left mastoid, G21 and G22, were used to measure movement artifact from the simulated scalp comprised of the wig coated with conductive gel placed over the swim cap. **b)** ERSP plots for the mastoid, G21, and G22 electrodes show similar broadband spectral fluctuations between 3–64 Hz.

Table 1

Mean ERSP correlation ± standard deviation across speeds for all nine subjects at channel A1.

	0.4 m/s	**0.8 m/s**	**1.2 m/s**	**1.6 m/s**
0.4 m/s	1	0.25 ± 0.13	0.02 ± 0.15	0.19 ± 0.16
0.8 m/s		1	0.08 ± 0.09	−0.04 ± 0.19
1.2 m/s			1	0.04 ± 0.12
1.6 m/s				1

Table 2

Mean ERSP correlation ± standard deviation across channels for all nine subjects at 1.2 m/s.

	A1	**A19**	**C18**	**E12**	**G11**
A1	1	0.47 ± 0.35	0.28 ± 0.34	0.38 ± 0.35	0.47 ±0.33
A19		1	0.53 ± 0.25	0.46 ± 0.38	0.43 ± 0.34
C18			1	0.41 ± 0.32	0.16 ± 0.28
E12				1	0.42 ± 0.29
G11					1

Table 3

Intersubject mean and standard deviation R-squared values for linear regressions using all three acceleration directions as variables for each electrode channel and speed.

Speed	Top (A1, Cz)	Back (A19)	Right (C18)	Front (E12)	Left (G11)
0.4	4.8 ± 9.1	6.2 ± 7.7	9.6 ± 11.1	9.5 ± 13.3	3.9 ± 4.6
0.8	15.1 ± 13.6	14.0 ± 12.8	23.2 ± 13.4	21.9 ± 12.7	21.7 ± 10.5
1.2	16.4 ± 10.9	16.5 ± 9.8	17.8 ± 7.0	13.8 ± 4.6	19.6 ± 10.9
1.6	13.0 ± 8.3	12.9 ± 9.4	18.0 ± 13.5	11.9 ± 11.6	15.4 ± 10.0